Desalination 549 (2023) 116321

Contents lists available at ScienceDirect

Desalination

journal homepage: www.elsevier.com/locate/desal

Experimental and economic evaluation of nanofiltration as a pre-treatment for added-value elements recovery from seawater desalination brines

Mariana Figueira [a,b,*], Daniel Rodríguez-Jiménez [a,b], Julio López [a,b], Mònica Reig [a,b], José Luis Cortina [a,b,c], César Valderrama [a,b]

[a] Chemical Engineering Department, Escola d'Enginyeria de Barcelona Est (EEBE), Universitat Politècnica de Catalunya (UPC)-BarcelonaTECH, C/Eduard Maristany 10-14, Campus Diagonal-Besòs, 08930 Barcelona, Spain
[b] Barcelona Research Center for Multiscale Science and Engineering, Campus Diagonal-Besòs, 08930 Barcelona, Spain
[c] CETaqua, Carretera d'Esplugues, 75, 08940 Cornellà de Llobregat, Spain

HIGHLIGHTS

- Nanofiltration experiments compared 3 membranes for desalination brine valorization.
- NF must be done before Ca removal stage at brine treatment for resource recovery.
- PRO-XS2 presented the highest selectivity between mono- and multivalent elements.
- Heating the brine for Ca removal jeopardizes the project's economic feasibility.
- Total levelized cost of 1.6 €/m^3 was estimated for Fonsalía plant brine.

GRAPHICAL ABSTRACT

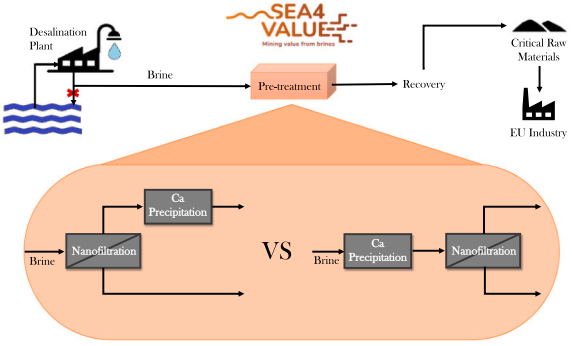

ARTICLE INFO

Keywords:
Sustainable brine mining
Circular economy
PRO-XS2
FilmTec Fortilife XC-N
FilmTec NF270
Desalination plant

ABSTRACT

Desalination brine mining emerges as a solution to supply raw materials to the European Union industry in a circular economy approach since valuable minerals and metals (e.g., B(III), Mg(II), Ca(II), Sc(III), V(V), In(III), Ga (III), Li(I), Mo(VI), Rb(I)) are present in seawater but in low concentrations. Brine pre-treatment is important to remove species that may impair the performance of other technologies involved and to increase recovery efficiencies. Hence, nanofiltration and calcium precipitation were proposed as pre-treatment stages. Nanofiltration was studied to separate monovalent from multivalent elements (Fonsalía desalination plant case study), while economically, it was evaluated whether it would be better to place it before (Scenario 1) or after (Scenario 2) a Ca(II) precipitation stage, considering that Ca(II) can produce scaling in membranes. Three commercial membranes were tested using synthetic brines at 30 bar. Experiments (65 % permeate recovery) showed that Fortilife XC-N and PRO-XS2 membranes presented higher Ca(II) and Mg(II) rejection than NF270. Heating the brine for Ca(II) precipitation jeopardizes the economic feasibility of the project. Scenario 1 was the best configuration since it presented lower total levelized cost (≈1.6 €/m^3 inlet, without heating the brine for Ca(II) removal). In such scenario, PRO-XS2 reported the best selectivity between monovalent and multivalent elements.

* Corresponding author at: Chemical Engineering Department, Escola d'Enginyeria de Barcelona Est (EEBE), Universitat Politècnica de Catalunya (UPC)-BarcelonaTECH, C/Eduard Maristany 10-14, Campus Diagonal-Besòs, 08930 Barcelona, Spain.
E-mail address: mariana.figueira@upc.edu (M. Figueira).

https://doi.org/10.1016/j.desal.2022.116321
Received 13 July 2022; Received in revised form 18 November 2022; Accepted 10 December 2022
Available online 26 December 2022

1. Introduction

It is estimated that >90 % of biodiversity loss and water stress [1] and 10 % of total greenhouse gas emissions (57.6 Gt CO_2 eq/y in 2018 [2]) come from resource extraction and processing. The transition to a circular economy model, where the life cycle of materials is extended and the waste is reduced to a minimum, is essential for European Union (EU) to develop a sustainable, low carbon, resource efficient and competitive economy [3]. Besides the environmental benefits, this transition gives competitive advantages by protecting businesses against scarcity of resources and volatile prices [4]. At the moment, the EU is lacking primary resources for several materials that are necessary for its economy, and the main input for them come from non-EU countries. To reduce the dependence on importations, the EU has created a list of Critical Raw Materials, which includes those elements of economic importance and high supply risk, such as borate, magnesium, and vanadium, among others [5]. This is aligned with the circular economy schemes that EU is promoting, as it aims to recover these critical materials from secondary sources.

In the last years, the concept of seawater mining has emerged, which is devoted to the recovery of critical raw materials from concentrated brines, such as seawater reverse osmosis (RO) brines [6]. Nowadays, about 74 % of global desalination installed capacity use RO technology [7]. RO is a pressure-driven membrane technology based on the use of a semi-permeable barrier that allows water transport while the permeation of salts is hindered. Therefore, purified water is obtained as permeate [8]. Nevertheless, the rejected brine (with approximately twice the concentration of the feed solution) is usually discharged into the sea, having adverse effects on the marine ecosystems. However, this brine can be used as a secondary source for the recovery of critical raw materials with a suitable selection of recovery technologies.

Searching for improved brine management strategies within the framework of circular economy and to promote the recovery of secondary raw materials from seawater, the European Union's Horizon 2020 Sea4Value project (https://sea4value.eu/) is under development. The project aims to recover valuable minerals and metals from seawater desalination plant (SWDP) brines, focusing on B(III), Mg(II), Ca(II), Sc (III), V(V), In(III), Ga(III), Li(I), Mo(VI), and Rb(I), most of them included in the EU's critical raw materials list. The project relies on three principles: to apply a circular supply model, to develop highly efficient separation technologies and, to integrate these and existing technologies into a multi-mineral modular brine mining process able to obtain multiple resources at the same time [9].

In recent decades, with the growth in the number of SWDPs, research related to the recovery of valuable raw materials from the brines generated has increased. However, most literature focus on species abundant in seawater (major elements, at g/L levels). Fewer studies have been published regarding the recovery of the minor (10 mg/L or less) minerals and metals present in brines (such as Li(II) [10], Rb(I) [11] and B(III) [12]). In this sense, Kumar et al. [13] performed an evaluation of the recovery of elements from seawater brine based on the market price of the element, extraction cost and concentration in brine. It resulted in the feasibility of extracting target elements such as B(III) and Rb(I), highlighting Mg(II) and Li(I) with greater economic potential, which are the ones that are expected to be recovered within the Sea4Value project. Khalil et al. estimate that worldwide about 1.5 million EUR are daily thrown back to the oceans as waste considering just the Li present in SWDP brine [14]. However, most of the published works are focused on extracting one or two elements and are still at initial level (lab-scale). The Sea4Value project (developed under the umbrella of EU through the Critical Raw Materials Action Plan) aims to bring these technologies to a higher technology readiness level (TRL) by developing a multi-mineral mining process.

It is worth commenting on the effect of low concentrations of elements in compromising the economic viability of extraction. In fact, the operating and maintenance costs of the extraction must be compensated with the recoverable amount of the element and its market price. In this regard, large flow rates are crucial for an affordable extraction of potentially profitable compounds, especially when market prices are also remarkably high. Shahmansouri et al. reported that elements such as Rb(II), Li(I), Si(IV), Sr(II) and Cs(I) would be profitable to extract for flow rates above 50,000 m^3/d. However, Rb(II) would be economically feasible to extract at flow rates below 5,000 m^3/d [15]. In addition, other authors reached similar conclusions stating that B(III) (1–10 ppm) and Li(I) (0.1 ppm) were within the limits of profitable elements for extraction. Other elements (Mo(VI), V(V) and Ga(III)) with higher market values but lower concentrations showed economic challenges to reach a profitable extraction [13].

The proposed pre-treatment of this brine mining process consists of a nanofiltration (NF) and a calcium removal stage. The pre-treatment is important to separate the elements into two streams to optimize their recovery (working with smaller volumes and higher concentrations is technically and economically advantageous) and to remove elements that may decrease the efficiency of the recovery downstream. NF is a pressure-driven membrane technology that hinders the transport of multivalent species, while the monovalent ones can permeate [16]. Indeed, the application of NF for the treatment of SWDP brines has been studied previously. For instance, Ali [17] proposed the use of NF as desalination brine pre-treatment for a series of RO stages in a zero liquid discharge configuration. Rejections of 98 %, 91 %, 54 % and 46 % were obtained for Mg(II), Ca(II), Cl(−I) and Na(I), respectively. Du et al. [18] developed and modeled a process train for NaOH production from SWDP brine using NF as pre-treatment. It was estimated that for 10,000 kt/year of brine treated, about 35,000 t/year of NaOH could be produced, increasing in 50 % the water recovery and reducing by 29 % the brine disposal at the desalination plant. These studies highlighted the possibility of NF for separating monovalent from multivalent elements in the permeate and concentrate respectively, for a further recovery process.

On the other hand, Ca(II) precipitation is commonly used as a pretreatment in SWDP brine valorization schemes, even more so if membrane technologies are used downstream [19]. In fact, the precipitation of Ca(II) insoluble salts (e.g., gypsum ($CaSO_4{\cdot}2H_2O$(s)) or calcite ($CaCO_3$(s))) may result in scaling [20]. The formation of inorganic salts may reduce the flow rate through the pipes, drop the efficiency of heat exchangers, and decrease the productivity of membrane and thermal processes [21]. Wang et al. [22] used a modified sodium carbonate method to remove Ca(II) from brine coming from seawater multi-effect membrane distillation. It was concluded that the factor with the highest impact in Ca(II) removal efficiency was temperature. At optimum operating conditions (85 °C, an equimolar dosage of sodium carbonate and brine salinity higher than 56 g/kg) it was possible to reach an efficiency of up to 85.4 % for Ca(II) removal, with a Mg(II) co-precipitation lower than 6.7 %. Chrisayu and Hanum [23] studied the extraction of Ca(II) from seawater in Indonesia (about 553 mg/L of Ca). After evaporating 50 % of the seawater and dosing 100 g/L oxalic acid, 99.99 % of the calcium precipitated. Therefore, under the appropriate circumstances, Ca(II) removal may be accomplished in order to avoid membrane scaling.

The objective of this work is to describe the relevance of NF as a pretreatment stage in a global process dedicated to the valorization of RO SWDP brines by recovering minerals and metals and to study the techno economic aspects of the proposed multimineral brine mining pretreatment including precipitation of Ca(II) and NF. To our knowledge, it could be the first process capable of recovering so many minerals simultaneously from SWDP brine. Thus, the NF performance of new commercial membranes (PRO-XS2 from Hydranautics and FilmTec Fortilife XC-N from Dupont), developed to enhance the rejections of multivalent ions in high-salinity media, was experimentally evaluated and the results were compared to those obtained by the traditional FilmTec NF270 from Dupont. It is worth mentioning that there are no previous studies on the performance of PRO-XS2, while only a few articles cover Fortilife XC-N [24], but none of them studied its

performance for brine treatment.

A Ca(II) precipitation stage in the pre-treatment train has been considered from the economic point of view. Nevertheless, it is necessary to consider that Ca(II) precipitation usually requires an increase in energy and chemicals consumption. However, capital and operational expenditures (CAPEX and OPEX, respectively) could be reduced if only the NF concentrate (about half the volume of original brine) feeds the Ca (II) precipitation stage. Thus, two scenarios were proposed: i) NF placed before the Ca(II) precipitation stage; and ii) to install the Ca(II) precipitation stage before the NF to avoid the potential scaling issues in NF. In this work, a case study was proposed for the Fonsalía (Canary Island) desalination plant, one of Sea4Value partners, evaluating both scenarios from a technical and economic point of view in order to evaluate the optimal configuration for the brine pre-treatment, prior to the metal and mineral recovery train.

2. Materials and methods

2.1. Case study: the seawater desalination plant in Fonsalía (Canary Islands)

The desalination plant in Fonsalía (Canary Islands) uses RO technology to produce 14,000 m^3/day of potable water. As its conversion rate is 40 %, the brine production is 21,000 m^3/day, which is currently discharged into the ocean at 225 m far from the coast [25]. This desalination plant could be considered a large scale SWDP since its production capacity is between 10,000 and 50,000 m^3/d [26]. However, extra-large RO SWDPs around the world now achieve capacities such as 330,000 m^3/d [27], reaching up to 600,000 m^3/d [28]. It is expected that a larger SWDP will be able to establish this trace element recovery approach due to economics of scale. Since the high fluxes of brines generated could balance out the critical lower concentration and eventually accomplish a feasible net production.

The two scenarios proposed for the pre-treatment are illustrated in Fig. 1, considering a permeate recovery of 65 % for NF (the same determined experimentally). However, only the pre-treatment stage of Sea4Value process is depicted in Fig. 1 due to confidentiality reasons. The subsequent stages include: advanced membrane crystallization, multi-effect distillation, ion-selective polymer inclusion membranes, bipolar membranes electrodialysis, adsorption and different solvent extraction techniques [9]. In scenario 1, only the multivalent-rich stream (i.e. concentrate) feeds the Ca(II) precipitation unit, which could save costs during the Ca(II) removal but would also increase scaling problems in the NF membrane. Meanwhile, in scenario 2 all the brine feeds the Ca(II) removal unit. Since the Ca(II) precipitation is performed with excess of $NaHCO_3$, scenario 2 needs a stage of acidification to avoid precipitation of carbonates, such as calcite and aragonite [29].

2.2. Reagents

For preparing the synthetic brine solutions that resemble the SWDP brines, anhydrous Na_2SO_4 (Glentham Life Sciences), $NaHCO_3$, NaCl, H_3BO_3, Li_2CO_3, Rb_2CO_3, In_2O_3, NH_4VO_3 (PanReac), KCl, $MgCl_2{\cdot}6H_2O$, Ga $(NO_3)_3$ (Alfa Aesar), Sc_2O_3, Na_2CO_3 (Sigma-Aldrich) and $(NH_4)_6Mo_7O_{24}$ (MERCK) were employed. All reagents were analytical grade.

Besides that, HNO_3 69 % from PanReac was used to condition samples for ICP and HCl 37 %, from the same supplier, was employed to

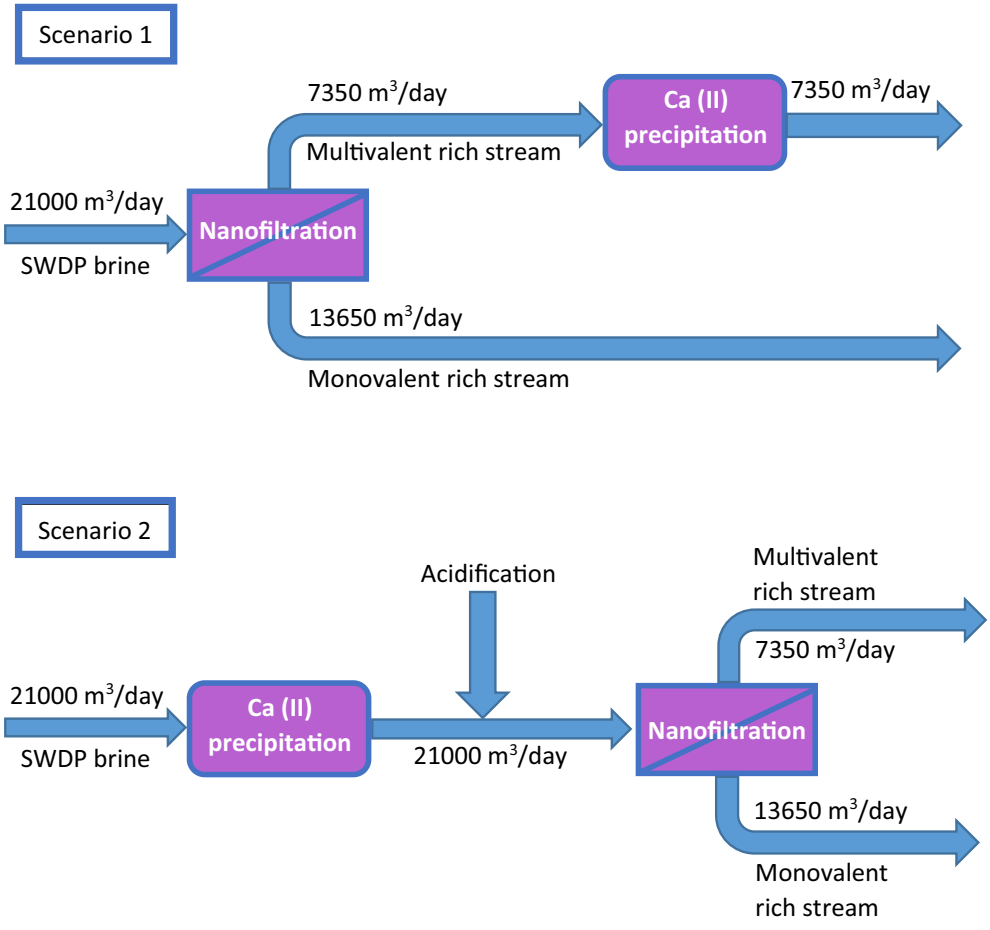

Fig. 1. Proposed brines pre-treatment within the scope of Sea4Value project.

adjust pH of the synthetic brine.

2.3. NF set-up

A flat-sheet experimental set-up was used to assess the performance of the three commercial thin-film composite NF membranes (PRO-XS2 from Hydranautics, FilmTec Fortilife XC-N and FilmTec NF270 from Dupont) for brine valorisation. Firstly, 8 L of synthetic brine solution were placed in the feed tank and isothermally maintained with a refrigerator at 25 ± 5 °C throughout the entire experiment. Furthermore, the high-pressure diaphragm pump (Hydracell, USA) variation frequency was set to 36 Hz. The feed solution was propelled inside a flat-sheet membrane module (GE SEPA™ CF-II) with an active membrane area of 0.014 m^2 and polypropylene spacers of 36 mil. Two pressure gauges were allocated at the feed and concentrate streams to monitor transmembrane pressure (TMP). Besides, TMP and flow were adjusted through a by-pass and needle valves. A flowmeter (Bürkert FLOW) measured the concentrate flow. Finally, a cartridge filter (10 μm) was placed in the concentrate stream to avoid corrosion particles from entering the pump.

2.4. Experimental methodology

The composition of the synthetic brine prepared was established after analysis of real brine samples coming from Fonsalía desalination plant (results of analysis presented in Table 1). Table 1 also lists the composition of the synthetic brines used in the experiments and compares it with SWDP brines from literature. The first brine (brine 1, pH 7.5) feeds the NF stage treating directly the brine coming from the SWDP (scenario 1). The second brine (brine 2) feeds the Ca(II) selective precipitation stage before the NF unit (scenario 2) thus, the original brine composition was modified accordingly. Molinari et al. [20] tested $Na_3C_6H_5O_7$, Na_2CO_3 and $NaHCO_3$ as calcium precipitation reagents for SWDP brine and reported better results for $NaHCO_3$ (reduced magnesium loss in the precipitated $CaCO_3$(s)). Hence, $NaHCO_3$ was selected in this study as precipitation reagent. The following assumptions were made to determine the composition of brine 2: $NaHCO_3$ was used in excess (10 %) to precipitate calcium, resulting on Ca(II) removal of 90 % and 10 % of Mg(II) removal [20]. Since the precipitation was performed with excess of $NaHCO_3$ there would be a concern related to the precipitation of carbonates that could also result in membrane scaling. Therefore, pH adjustment would be necessary to avoid precipitation of $CaCO_3$(s) [29]. A simulation was performed with PHREEQC software for brine 2 composition, at pH 6.5 (presented in Fig. A.1 — Supplementary Information) and it was determined that there would be a risk of gypsum precipitation ($CaSO_4{\cdot}2H_2O$(s)), but there would not be precipitation of aragonite and calcite (polymorphs of $CaCO_3$(s)) for % permeate recovery below 80 %. Therefore, the pH was set to 6.5 in brine 2 to avoid carbonates precipitation. Due to the low concentration of Li(I), In(III), Rb (I), V(V), Ga(III), Sc(III) and Mo(VI) in the SWDP brines (μg/L levels), it was decided to spike their concentrations to 0.5 mg/L to make them measurable by the analytical techniques in order to determine clearly the rejection trends.

Initially, simulations carried out with the WAVE software from Dupont [34] with the membrane NF270 determined that to achieve a permeate recovery of 65 %, the feed pressure had to be set at 30 bar (results from the simulation are included in Table B.1 — Supplementary Information). Therefore, a pressurization stage at 32 bar and 5 L/min (crossflow velocity of 1 m/s) was performed before each experiment. Initially, distilled water was used followed by pressurization with the brine in a closed-circuit configuration (recirculation of permeate and concentrate). Then, the experiments were performed in open-circuit, hence the concentrate obtained from the NF module was recycled into the feed tank, while the permeate was extracted out of the system. In this way, it was possible to simulate several NF modules in series. Experiments were performed at constant TMP (30 bar) and feed flow (3.5 L/min, crossflow velocity of 0.7 m/s) until 65 % permeate recovery was achieved. Concentrate and permeate samples were collected at the beginning of the experiment and after recovering 0.25 L of permeate. Conductivity, pH and temperature were monitored in all samples.

2.5. Analytical methodologies

Samples were analyzed by ionic chromatography (DIONEX AQUION) with the aim of determining Cl^- and SO_4^{2-} concentrations. Precisely, a DIONEX-ADRS 600 column and 25 mM KOH as mobile phase were used. Moreover, carbonate concentration was determined by automatic titration (Mettler Toledo T70 — Rondolino) using 1 mM HCl solution as titrant. Finally, concentrations of the other elements in solution were determined by spectrometry (7800 inductively coupled plasma mass spectrometry (ICP-MS) and 5100 inductively coupled plasma optical emission spectrometry (ICP-OES) from Agilent Technologies). Conductivity and pH of samples were determined on-site via a pH-meter (CRISON GLP-22) and a conductimeter (CRISON GLP-31).

2.6. Experimental data analysis

For the calculation of rejections (R(%)), Eq. 1 was employed using the permeate (c') and feed concentrations (c^f).

$$R(\%) = \left[1 - \frac{c'}{c^f}\right] \cdot 100 \quad (1)$$

Likewise, concentration factors (CF) and permeate recoveries (% p. r.) were calculated through Eqs. 2 and 3, respectively, where c'' is the

Table 1
Brines composition (mg/L) simulating the composition for the two proposed scenarios and comparison among different brines composition found in literature.

Major elements	Predominant species [30]	Concentration (mg/L)					
		Brine 1	Brine 2	Fonsalía	Atlantic [31]	Mediterranean [32]	Red sea [33]
Na(I)	Na^+	21,690.63	21,823.99	21,700	25,237	27,521	21,432
S(VI)	SO_4^{2-}	5,667.63	5,667.63	5,665	6,050	–	5,326
K(I)	K^+	801.51	801.51	800	781.82	554	1,034
Cl(−I)	Cl^-	39,634.67	39,634.67	37,931	41,890	–	40,890
Inorganic carbon (IC)	HCO_3^-/CO_3^{2-}	24.17	53.38	24.17	1,829.00	–	227.00
Mg(II)	Mg^{2+}	2,803.78	2,523.07	2,802.51	2,867.00	2,450.00	2,128.50
Ca(II)	Ca^{2+}	860.35	86.02	864.45	960	–	713
B(III)	H_3BO_3	8.45	8.45	8.45	8.00	4.45	–
Li(I)	Li^+	0.50	0.50	0.41	–	0.27	–
In(III)	$In(OH)_3$	0.50	0.50	0.04	–	0.02	–
Rb(I)	Rb^+	0.50	0.50	0.29	–	0.19	–
V(V)	$VO_2(OH)_2^-/VO_3OH^{2-}$	0.50	0.50	0.004	–	–	–
Ga(III)	$Ga(OH)_4^-$	0.50	0.50	0.0006	–	–	–
Sc(III)	$Sc(OH)_3$	0.50	0.50	0.006	–	–	–
Mo(VI)	MoO_4^{2-}	0.50	0.50	0.02	–	–	–

concentration at the concentrate stream and V' and V^f are the permeate and feed volumes (L), respectively. A plunging in rejections is expected as more permeate is recovered due to a progressive concentration of the feed (only the concentrate was recirculated to the feed tank), which can be related to: i) a decrease in the permeate flux at higher % p.r. due to the increase in the osmotic pressure of the feed solution, and ii) a higher concentration gradient across the membrane, resulting both in a decrease in rejections [35].

$$\mathrm{CF} = \frac{c'^{\prime}}{c^f} \tag{2}$$

$$\%\mathrm{p.r.} = \left[\frac{V'}{V^f}\right]\cdot 100 \tag{3}$$

To obtain the permeate flux (J_v, LMH), Eq. 4 was used in which A (m^2) and t (h) stand for membrane area and sample-collecting time respectively.

$$J_v = \frac{V'}{A\cdot t} \tag{4}$$

In addition, average selectivity factors ($\overline{SF}$) along p.r. between monovalent species and multivalent species on every membrane were calculated using Eq. 5, where $\overline{R}_{mon}$ and $\overline{R}_{multi}$ are the average rejection along p.r. of the average monovalent group and multivalent group, respectively.

$$\overline{SF} = \frac{100 - \overline{R}_{mon}}{100 - \overline{R}_{multi}} \tag{5}$$

2.7. Economic evaluation assumptions

The two scenarios proposed in Fig. 1 were considered for the estimation of CAPEX of the brine pre-treatment. The Fonsalía desalination plant produces about 21,000 m^3/day of brine. Adel et al. [36] reported that the permeate flow in a RO desalination plant can decrease by 25 % between two cleaning-in-place (CIP) procedures. As 21,000 m^3/day was considered an average value, it was assumed that the production of the desalination plant could range between 24,000 and 18,000 m^3/day approximately. The permeate production in the NF for 65 % p.r. (maximum value obtained experimentally) was estimated to be 13,650 ± 2,000 m^3/day or 569 ± 83 m^3/h for both scenarios.

Ning [37] reported that a complete NF system that produces 226 m^3/h of permeate (with a p.r. of 65 %, using 29 pressure vessels with 6 membrane elements in each vessel, at 25 bar) had a CAPEX of 1.2 million 2015EUR including direct and indirect costs, but excluding the cost of pressure vessels and membrane elements. This cost was updated to 2021 (1.3 million 2021EUR) based on the inflation rate for the period of time. Eq. 6 was used to calculate the inflation rate in Spain for the period.

$$\text{Inflation Rate}\ (\%) = \frac{\mathrm{CPI}_{\text{final year}} - \mathrm{CPI}_{\text{initial year}}}{\mathrm{CPI}_{\text{initial year}}} \times 100 \tag{6}$$

where CPI is the consumer price index. The annual average (CPI 2021 = 100 since it was the base year and CPI 2015 = 93.4) of general CPI calculated by the Spanish National Institute of Statistics was used [38]. Then, a cost correlation was used (Eq. 7) to determine the NF CAPEX (excluding pressure vessels and membrane elements) based on the reference value, where n is the correlation parameter that depends on the equipment considered. The smaller the value of n, the more advantageous is the scale-up [39]. A typical value of n for RO/NF systems is 0.85 [39],

$$\mathrm{Cost}_{\text{case study}} = \mathrm{Cost}_{\text{reference}}\left(\frac{\mathrm{Size}_{\text{case study}}}{\mathrm{Size}_{\text{reference}}}\right)^n \tag{7}$$

For the calculation of number of membrane elements (membranes) needed in this case study, Eq. 8 was used, where Q_p (L/h) is the total permeate flow rate, J_v (LMH) is the average volumetric flux obtained experimentally for each membrane and A_e (m^2) is the active membrane area of one element. The active membrane area of one element was considered 37 m^2 for NF270-400/34i [40] and for PRO-XS2 [41], and 34 m^2 for Fortilife XC-N [42].

$$\text{number of elements} = \frac{Q_p}{J_v A_e} \tag{8}$$

For the Ca(II) precipitation stage, the work of Molinari et al. [20] was considered. The synthetic brine used by the authors had the same concentration of major elements as the brine 1 used in this work (corresponding to scenario 1). It was concluded that the optimal conditions to obtain the maximum Ca(II) removal were obtained using $NaHCO_3$ with a molar ratio HCO_3^-/Ca(II) = 3 and temperature of 60 °C. The CAPEX for the Ca(II) precipitation was calculated according to Chen et al. [43], who considered indirect costs as 10 % of direct costs. The flow rate feeding this stage (about 21,000 m^3/day for scenario 2 and 7,350 m^3/day for scenario 1) was considered in Eq. 7 to calculate the CAPEX using $n = 0.49$, typical of precipitation systems [39].

On the other hand, membrane scaling could significantly reduce productivity and permeate quality, increasing the frequency of membrane cleaning and reducing membrane lifespan [44]. The reduction of membrane lifetime could increase the OPEX of the project. It is expected that with scenario 2 (see Fig. 1), the previous removal of Ca(II) would decrease membrane scaling and increase NF membrane lifetime. The replacement of membranes is typically 5 to 10 years [45]. Since Ca(II) precipitation is the main issue regarding membrane scaling in this case, it was assumed that for scenario 1 the lifetime of membranes was 5 years while for scenario 2 it was 8 years.

An in-line acidification system in scenario 2 was proposed to reduce the brine pH to 6.5, before the NF technology. This proposed system should not induce significant changes in CAPEX, but the consumption of HCl is significant for OPEX estimation. The consumption of HCl was based on the NF experiments where about 45 mL of HCl 37 % (pure) were required to decrease the pH of 30 L of the synthetic brine 2 to 6.5 (Section 2.4). With a simple direct correlation between volumes and considering the density of the solution as 1.19 kg/L, the mass of HCl 37 % solution necessary to adjust the pH of 21,000 ± 3,000 m^3/day of brine was estimated (37,485 ± 5,000 ton/day). Still related to OPEX, the maintenance cost was supposed to be 3 % of CAPEX [46]. For the labor cost, it was presumed that 2 supervisors and 6 operators were necessary.

Eq. 9 was used to calculate the capital charge factor [47], where r is the interest rate and m is the plant lifetime. An interest rate of 5.5 % was assumed for a conservative approach since 5.5 % was the highest value in the past 20 years in Spain (currently the interest rate is 3 %) [48]. The total cost including CAPEX and OPEX was levelized using the capital charge factor and normalized by the inlet flow of SWDP brine [49].

$$\text{capital charge factor} = \frac{r(1+r)^m}{(1+r)^m - 1} \tag{9}$$

Finally, the specific energy consumption (SEC) is the amount of energy needed to produce a unit volume of permeate, expressed in kWh/m^3 [50]. For the calculation of SEC, Eq. 10 was used [51]:

$$\mathrm{SEC} = \frac{Q_f \mathrm{TMP}}{36 Q_p \eta} \tag{10}$$

where Q_f (L/h) is the feed flow rate and η is the efficiency of the pump, which was assumed to be 0.80. Table 2 summarizes the main assumption used at the economic evaluation.

3. Results and discussion

3.1. Technical NF results considering the NF step prior to Ca(II) precipitation (scenario 1)

3.1.1. Major elements

The rejection values obtained with the NF set-up for the elements in major and minor concentration in brine 1 (no calcium removal pre-treatment before NF) are depicted in Fig. 2. It was targeted to achieve with the new membranes (Fortilife XC-N and PRO-XS2) rejections higher for multivalent and lower for monovalent elements than the rejections reported in literature for NF270 (Ca(II) = 50 %, Mg(II) = 71 %, NaCl = 12 %, K(I) = 5 % and S(VI) = 91 % [57]).

As a result, NF270 membrane fed with brine 1 showed markedly differences in major divalent elements (Fig. 2a). Indeed, S(VI) was the most rejected element (85 %), followed by Mg(II) and Ca(II), being rejected 75 % and 60 %, respectively. It is worth mentioning that S(VI) was present in the solution as SO_4^{2-}, then it was the most rejected ion due to Donnan exclusion, one of the governing hindered mechanisms in NF. Precisely, polyamide Thin-Film Composite (TFC) NF membranes surface arises an electric field depending on pH due to the protonation/deprotonation of the amino and carboxylic free radicals in the active layer. Above isoelectric point (IEP), membranes acquire negative charge. For example, the IEP of the membrane NF270 is in the range of pH from 3.00 to 4.05 for 1 to 50 NaCl mol/m^3 [58]. Thus, counter-ions might permeate easier than co-ions due to charge attraction/repulsion. Then, Donnan exclusion explains the fact that cations such as Ca^{2+} and Mg^{2+} were less rejected than anions (e.g., SO_4^{2-}), for pH above IEP [59].

Regarding the monovalent elements (Na(I), Cl(−I), K(I), IC), their rejections were around to 20 %, 30 %, 35 % and 47 %, respectively for NF270. These rejections, in contrast to divalent species could be explained by the second governing exclusion mechanism: dielectric exclusion [60]. Due to the difference of dielectric constants between solution and the polymeric matrix, the ions in solution must lose the hydration shell, which is proportional to the square of the absolute charge of the ions [61]. Therefore, it was expected that multi-charged species were more repelled than mono-charged/non-charged ones.

Furthermore, a declining trend in rejections, as more permeate recovery (p.r.) was obtained, was another key aspect shared barely among some major elements. In fact, as it can be seen in Fig. 2a rejections for Mg(II), IC, K(I) and Cl(−I) lowered from 78 %, 51 %, 34 % and 30 % at 0 % p.r. to 68 %, 43 %, 24 % and 21 % at a 66 % p.r., respectively. Unlikely, the rest of species maintained a constant tendency along the p.r. and even though some declining trend was observed, it was not steeper enough to assure a diminish in rejections. Overall, divalent elements (Mg(II)) shrinkage in rejections only achieved a 12 % drop while monovalent (K(I) and Cl(−I)) lowered their rejections in 30 % at maximum levels of % p.r.. The explanation that covers exclusion mechanisms justifies various shrinking trends in rejections between monovalent and multivalent. As mentioned, more permeate recovered means a more concentrated feed because only the concentrate stream was recirculated back to the feed tank. As a result, a greater concentration gradient raised and due to Fick's law of diffusion, species permeated trough the membrane easily and rejections gradually decreased. Nevertheless, dielectric exclusion influence is more severe in multivalent species rejections than in monovalent. Thus, even with a steeper concentration gradient that lowers rejections, multivalent rejections dropped at a smoother slope than monovalent ones.

Regarding Fortilife XC-N performance in major elements rejections (Fig. 2c), the following average values were obtained for Ca(II), Mg(II) and S(VI): 78 %, 83 % and 77 %, respectively. In contrast to the high rejection for divalent element, monovalent ones had their rejections distributed between 30 % for K(I) to 13 % for both Cl(−I) and Na(I). On the other hand, IC showed mild-high rejections (50 % on average). The wide gap in rejections that was laid between divalent and monovalent elements strengthen the hypothesis that dielectric exclusion had greater influence than Donnan exclusion when evaluating the rejection of species by NF membranes. In addition, again most of the species exhibited a notably diminishing trend in rejections as % p.r. increased. Rejections of Ca(II), Mg(II) and S(VI) (divalent species), that were 83 %, 88 % and 81 % at 0–10 % p.r. decreased to 69 %, 75 % and 75 % at maximum permeate recovery achieved (65 %), respectively. Meanwhile, monovalent species (IC, K(I), Na(I), Cl(−I)) showed a drop in rejections from 57 %, 30 %, 28 % and 21 % to 49 %, 22 %, 15 % and 13 %, respectively. Furthermore, the relative falls (%) in rejections per element uncovered the fact that monovalent (14 %, 26 %, 46 % and 38 %) suffered more serious declines that divalent elements (16 %, 14 % and 7 %).

Concerning major elements rejection when using PRO-XS2 (Fig. 2e), divalent species such as Ca(II), Mg(II) and S(VI) showed average rejections around 70 %, 86 % and 90 %, respectively. Among the divalent group, it could be observed that Ca(II) achieved rejections values below the ones for Mg(II) and S(VI) for all the p.r. studied range. Precisely, it was stated a 20 % rejection gap among them. Moreover, since S(VI) dominant species was SO_4^{2-} at experimental pH conditions, its high rejection was easily explained as a resultant combination of Donnan and dielectric exclusions. In contrast, monovalent elements reached considerably low rejection values between 33 % and 20 %. Average rejections obtained for K(I), Na(I) and Cl(−I) were 23 %, 27 % and 31 %, respectively, although IC showed higher rejections (64 % on average). Consequently, due to dielectric exclusion, monovalent and divalent elements (excluding IC) were separated by a rejection gap of about 30 %. Regarding the expected decline in rejections as more permeate was extracted, a slight general downward trend could be perceived. In exception of Mg(II) and Ca(II) of which rejections shrunk from 89 % and 73 % to 83 % and 65 % at a 67 % p.r., respectively.

3.1.2. Minor species

Referring to NF270 performance on rejecting minor species (Fig. 2b), multivalent species (i.e. Sc(III), In(III), Ga(III), Mo(VI) and V(V)) were highly rejected (80–100 %). As showed in Table 2, it is worth mentioning that Sc(III) and In(III) rejections will be explained in the multivalent group even though both elements are present as a non-charged species. The explanation lays in a strong size exclusion due to a coordination of hydroxyl ions and water with the central ion. For instance, it could be observed experimentally that $In(OH)_3$ adopted an octahedral structure in coordination with 3 water molecules and 3 hydroxy ions ($[In(H_2O)_3(OH)_3]^0$) [62]. In addition, due to dielectric exclusion as the most influent exclusion mechanism, multivalent elements showed higher rejections in comparison to monovalent (i.e. Rb(I) and Li(I)) and non-charged species (such as B(III) in the form of boric

Table 2
Main assumption used for the economic evaluation (€ = 2021EUR).

Fonsalía SWDP brine production (m^3/day)	21,000 ± 3000	[25]
Cost of NF system excluding pressure vessels and membranes (M€)	2.9 ± 0.4	[37]
NF membrane cost (€/m^2)	40	[52]
Cost of each pressure vessel (€)	963	[37]
Cost of Ca(II) crystallizer (M€)	0.27 ± 0.02 for scenario 1 and 0.46 ± 0.03 for scenario 2	[43]
$NaHCO_3$ cost (€/ton pure)	350	[53]
HCl cost (€/ton pure)	140	[54]
Supervisor salary in Spain (€/year)	43,561.40	[55]
Operator salary in Spain (€/year)	16,438.27	[55]
Interest rate (%/year)	5.5	[48]
Plant lifetime (years)	20	[49,56]
Capital charge factor (%/year)	8.4	Derived from the two previous assumption (Eq. 9)

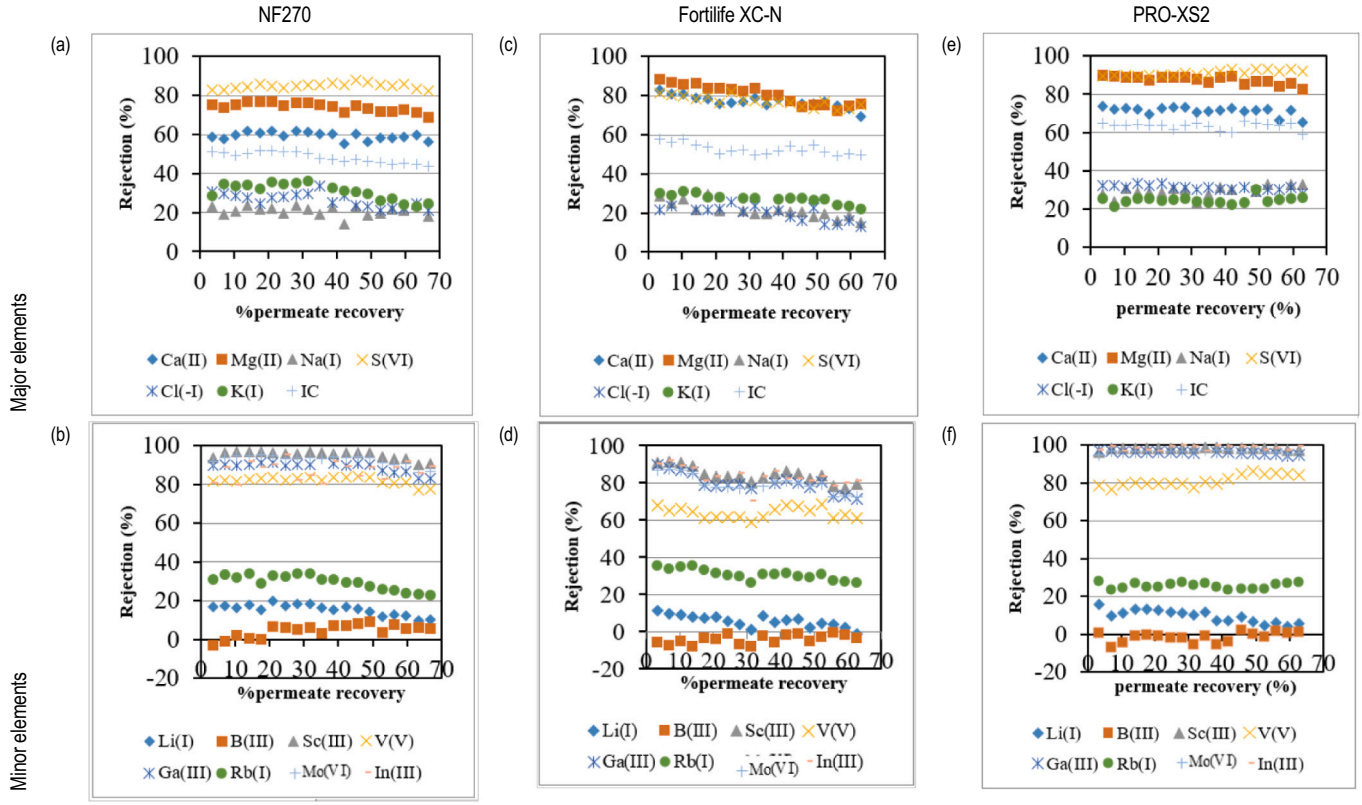

Fig. 2. Permeate recovery influence on minor and major rejection profiles for brine 1: a) NF270 major species; b) NF270 minor species; c) Fortilife XC-N major species; d) Fortilife XC-N minor species; e) PRO-XS2 major species; f) PRO-XS2 minor species.

acid at pH below 9.24, i.e. H_3BO_3(aq) [63]), that exhibited rejections at least 45 % lower than the multivalent ones. Moreover, Rb(I), Li(I) and B (III) were found within the low-rejected elements achieving average rejections of 30 %, 16 % and 3 %, respectively. B(III) showed the lowest rejection because the electromigration exclusion mechanisms did not influence it as a non-charged specie. About the fall on rejections due to an increment in feed concentration, a slight trend was observed in multivalent elements. Nevertheless, a gradual drop on Rb(I) and Li(I) was exhibited from 31 % and 17 % to 23 % and 10 %, respectively at 67 % p.r. The relative decrease in rejections was around 25 % and 41 % of initial rejection values.

In experiments with the Fortilife XC-N membrane (Fig. 2d), multivalent elements registered elevated rejections that were sustained along the % p.r. and comprised rejections between 90 and 70 %. However, V (V) showed lower rejection (64 %) than the rest of multivalent. In fact, V (V) in solution at the experimental pH was expected to be a mixture of $VO_2(OH)_2^-$ and VO_3OH^{2-}, as indicated by the speciation diagram of V(V) done with the Hydra/Medusa software [30] presented in Supplementary Information, Fig. C.1. As a result of its presence as a monovalent species, rejections were expected somewhat lower than multivalent ones. Unlikely to multivalent ions, a compact rejection range was not reached by monovalent elements since Rb(I) was rejected around 30 %, while Li(I) and B(I) were 5 % and −5 %, respectively. Besides, Sc(III), In(III), Mo (VI), Ga(III), V(V), Rb(I) and Li(I) exhibited a shrinkage in rejections as more permeate was recovered dropping from 90 %,90 %, 86 %, 89 %, 67 %, 35 % and 11 % at 3 % p.r. to 79 %, 81 %, 72 %, 71 %, 60 %, 26 % and −3 % at 62 % p.r., respectively. Nevertheless, this trend could not be observed for B(III) as its rejections were on average close to 0 %. In other words, relative fall on rejections for Sc(III), In(III), Mo(VI), Ga(III), V(V), Rb(I) and Li(I) were the following: 12 %, 10 %, 16 %, 20 %, 10 %, 25 % and 125 %. As a result, it could be inferred that monovalent elements tended to suffer more serious declines in rejections.

On the results of the PRO-XS2 membrane (Fig. 2f), multivalent were highly rejected and even V(V) rejections were above 80 %. Additionally, Sn(III), In(III), Mo(VI), Ga(III) rejections were all comprised above 95 % and in some occasions, extremely close to 100 %. As a result, such high rejections created a remarkable wide gap in rejections between monovalent and multivalent. In monovalent group, Rb(I) rejections were around 25 % while Li(I) and B(III) were approximately 10 % and −2 %, respectively. In addition, no remarkable falls were observed on rejections as %p.r. was increased, except for Li(I), whose rejections lowered from 15 % to 5 % at the maximum % p.r. achieved (62 %).

3.2. *Technical NF results considering the NF step after Ca(II) precipitation (scenario 2)*

3.2.1. *Major elements*

The rejection values obtained with the NF set-up for the elements in major and minor concentration in brine 2 (calcium removal pretreatment before NF) are shown in Fig. 3.

Concerning NF270 results with brine 2, multivalent elements such as Ca(II), Mg(II) and S(VI) showed rejections close to 60 %, 70 % and 83 %. As it can be seen in Fig. 3a, multivalent elements did not form a narrow rejection range and between each three elements laid a significant 10 % gap. Once again, S(VI) was the most rejected element because of an intense influence of electric exclusion mechanisms on its main specie (SO_4^{2-}). Along the same scenarios, a compact rejection group within monovalent elements could not be achieved since Cl(−I) and IC rejections remained slightly higher (50–55 %). Meanwhile, Na(I) and K(I) rejections were low (~20 %) as expected due to their single positive charge. Moreover, a dropping tendency on rejections as more permeate was recovered was observed for Mg(II), S(VI) and Cl(−I). Concretely, their rejections shrunk from 80 %, 91 % and 54 % to 67 %, 79 % and 37 % at maximum p.r. (67 %). Among these three elements, the multivalent (Mg(II) and S(VI)) showed less pronounced declining (13–16 %) than the monovalent (31 % rejection for Cl(−I)).

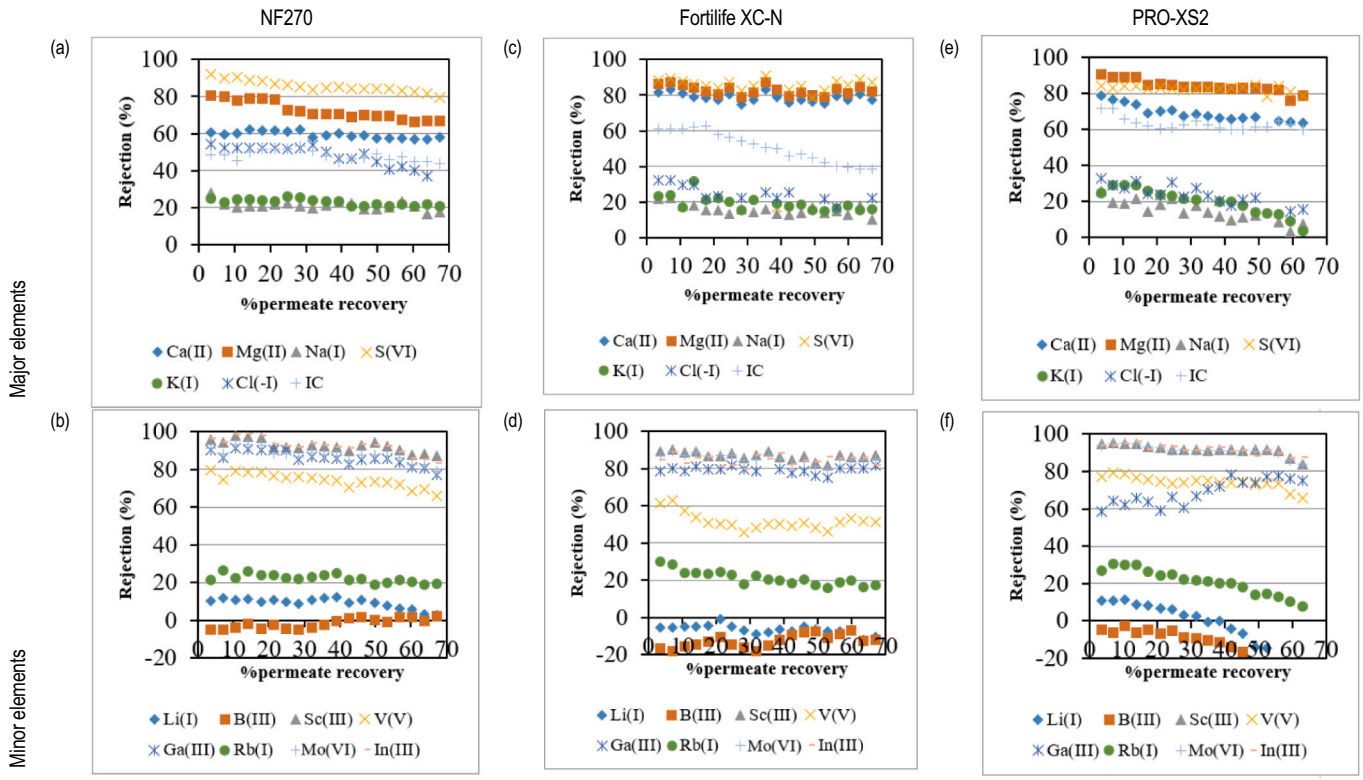

Fig. 3. Permeate recovery influence on minor and major rejection profiles for brine 2: a) NF270 major species; b) NF270 minor species; c) Fortilife XC-N major species; d) Fortilife XC-N minor species; e) PRO-XS2 major species; f) PRO-XS2 minor species.

With regard to Fortilife XC-N (Fig. 3c), Ca(II), Mg(II) and S(VI) showed close rejections comprised in a gap ranging from 75 to 90 %. On average, 77 %, 81 % and 85 %, respective rejections were achieved. Furthermore, S(VI) was the most rejected specie as expected due to the exclusion mechanism mentioned before. Also, IC was the most rejected monovalent element with a rejection of 50 %, still bellow multivalent elements rejections. Nevertheless, the rest of monovalent (K(I), Cl(−I) and Na(I)) rejections were even lower and more compact (35–15 %). Precisely, their average rejections were 22 %, 25 % and 15 %. In this scenario, a declining trend on rejections could mainly be observed in monovalent elements. In that way, K(I), Cl(−I) and Na(I) decreased from 23 %, 32 % and 21 % to 15 %, 22 % and 10 % at 67 % p.r. Moreover, relative shrunk on rejections were the following: 34 %, 31 % and 52 % for K(I), Cl(−I) and Na(I). Unlike, divalent rejections seemed to barely drop.

About PRO-XS2 (Fig. 3e), divalent Mg(II) and S(VI) were rejected on average approximately (83 %) and showed rejected profiles remarkably similar. In contrast, Ca(II) was rejected substantially less (68 %) than both divalent Mg(II) and S(VI). On the bottom of rejections, monovalent ones comprised a compact group of rejected species (between 32 % and 3 %) with average rejections for K(I), Na(I) and Cl(−I) of 21 %, 14 % and 23 %, respectively. Nevertheless, IC showed higher rejections (>60 %).

3.2.2. *Minor species*

In the experiment using the NF270 membrane (Fig. 3b), Sc(III), In (III), Mo(VI) and Ga(III) showed rejections particularly high (~90 %) conforming a high-rejected compact group. However, V(V) was not so highly rejected (70 %) due to its speciation as an equimolar mixture of $VO_2(OH)_2^-$ and VO_3OH^{2-}. Contrary to high-rejected elements, monovalent ones comprised a group of low rejected elements located below a 45 % rejection gap from V(V). As a result, monovalent elements were remarkably separated in rejections in comparison to multivalent ones. Furthermore, Rb(I), Li(I) and B(III) had average rejections of 22 %, 9 % and −4 %. B(III) showed fundamentally negative rejections. Since B(III) is neutral-charged due to its speciation (see Fig. C.2 — Supplementary information), it is not repelled by electric fields generated by the membrane. And as the permeate volumetric flux is way lower than the feed volumetric flow, depending on molecules electromigration it could happen that a greater permeate concentration is achieved in comparison with the feed concentration of boron [64]. Additionally, an undeniable shrunk on rejections appeared for all species regardless B(III). Sc(III), In (III), Mo(VI), Ga(III) and V(V) fell from 95 %, 97 %, 91 %, 91 % and 79 % to 87 %, 83 %, 79 %, 79 % and 66 % at a 67 % p.r.. In contrast, monovalent Rb(I) and Li(I) had a drop from 26 % and 10 % to 19 % and 2 %, respectively. Moreover, it could be observed that multivalent elements (Sc(III), In(III), Mo(VI), Ga(III) and V(V)) had an 8 %, 14 %, 13 % and 16 % relative decreasing on rejections from their initial value. Meanwhile, monovalent (Rb(I) and Li(I)) showed deeper falls (27 % and 80 %, respectively).

Fortilife XC-N (Fig. 3d) caused noticeably high rejections on Sc(III), In(III), Ga(III) and Mo(VI), that showed average rejections of 85 %, 85 %, 80 % and 82 %, respectively. However, V(V) rejections were way lower than multivalent ones (50 %). Regarding monovalent elements, a wide gap in rejection appeared between Rb(I) (20 %), Li(I) (−7 %) and B (III) (−15 %). Moreover, remarkable decreasing trends were observed in Rb(I), as it rejections shrunk from 30 % to 17 % at a 67 % p.r. Furthermore, a subtle decreasing tendency in V(V) appeared lowering its rejections from 61 % to 51 %.

Assessing PRO-XS2 performance in multivalent elements (Fig. 3f) showed overlapped rejections from Sc(III), In(III) and Mo(VI) (around 90 %). In addition, V(V) rejections were scattered around 65 and 80 %. And Ga(III) showed its rejections comprised between 58 and 78 %. About monovalent elements, all presented low rejections since Rb(I), Li (I) and B(III) were rejected on average 21 %, 2 % and 10 %, respectively. In fact, both Li(I) and B(III) acquired negative rejections after a 30 % p. r., reaching rejection values slightly below −20 % at the highest % p.r. (62 %).

3.3. Comparison among the membranes and scenarios tested

Overall, the new commercial membranes PRO-XS2 and Fortilife XC-N presented a higher rejection of Ca(II) and Mg(II) than the traditional commercial membrane NF270. For example, while NF270 presented Ca (II) rejections below 60 % at 65 % p.r. for both scenarios, PRO-XS2 reached 65 % Ca(II) rejection and the values for Fortilife XC-N were even higher than 70 %. Regarding Mg(II), the rejections at 65 % p.r. were about 70 % for NF270 in both scenarios, 75 % and 83 % for Fortilife XC-N and 85 % and 78 % for PRO-XS2 in scenarios 1 and 2, respectively. Considering major elements in scenario 1, PRO-XS2 was the membrane whose rejections varied the least with the increase in %p.r., while in scenario 2 the performance of Fortilife XC-N was more constant independently on % p.r.

Regarding the minor elements, Fortilife XC-N and NF270 presented similar behavior for scenarios 1 and 2 while the rejection profile of PRO-XS2 changed considerable. In scenario 1 the rejection of Sc(III), In(III), Mo(VI) and Ga(III) given by PRO-XS2 was always above 95 %. Nevertheless, in scenario 2 the rejections of Sc(III), In(III) and Mo(VI) reached 85 % and Ga(III) 78 % at 65 % p.r. The value of 85 % was higher than that obtained with other membranes, however in the case of Ga(III), PRO-XS2 presented lower rejections than the other membranes. Overall, PRO-XS2 was the best membrane for separation of minor monovalent and multivalent elements in scenario 1 but in scenario 2 NF270 had a better performance.

The obtained results were compared with those previously published in the literature. It must be highlighted that in most of the cases, the studies published referring to the treatment of seawater or SWDP brines do not focus on the behavior of minor elements. Liu et al. [65] performed similar experiments regarding the influence of permeate recovery on seawater brine elements rejections using NF. A DL2540 (GE Co. Ltd.) spiral wound membrane was used to assess the rejections behavior considering the following feed composition in mg/L: Na(I): 20,520; Ca (II): 630; Cl(−I): 36,900; K(I): 830; S(VI): 5,200; Mg(II): 2,480; IC: 240. Initially, rejections (%) at 12 bar were as follows: 0, 60, 10, 8, 100, 92 and 30 for Na(I), Ca(II), Cl(−I), K(I), S(VI), Mg(II) and IC, respectively. However, at maximum p.r. obtained (54.3 %) at 12 bar and 7.33 L/min inlet flowrate, rejections decreased noticeably for Mg(II) and Ca(II) to 37.8 % and 87.8 % respectively, while the same dropping trend was observed for Cl(−I), K(I) and Na(I), whose rejections reached a bottom at 5 %.

In addition, a double-stage NF and electrochemical disinfection was proposed by El-Ghzizel et al. [66] to produce drinking water from local underground water (Kenitra, Morocco) using NF90 spiral-wound membranes (DuPont). Concerning the double-stage NF process, the following rejections (%) were reported at 75 % p.r. at 5 bar and 7.66 L/min inlet flowrate: K(I): 78.6 %, Na(I): 84.4 %, Mg(I): 96.3 %, Ca(I): 92.9 %, IC: 92.3 %, Cl(−I): 96 % and S(VI): 96.5 %. Nativ et al. [67] studied a hybrid 6NF monovalent selective and RO process with the aim of desalinating brackish water using the following composition (in mg/L): Ca(II): 188; Mg(II): 166; Na(I): 1,118; and Cl(−I): 2,269. Their experiments were performed at 6 bar in a pilot-scale plant formed by 1 module of 4 GE DL-4040-F1021 Stinger membranes. Under the tested conditions, it was possible to recover 70 % of water as permeate, obtaining overall rejections of 52.6 %, 69.9 %, 10.4 % and 14.4 for Ca (II), Mg(II), Na(I) and Cl(−I), respectively.

Scarce studies were found focused on analyzing NF rejections of all the minor elements considered in this work when treating SWDP brine. For instance, Somrani et al. [68] studied the separation of Li from salt lake (Chott Djeri, Tunisia) brines using NF. Using the 10-fold diluted brine (340 mg/L of Mg(II) and 6 mg/L of Li(I)), the polyamide TFC membrane NF90 by Filmtec (Dupont) was used to separate Li(I) from Mg (II). The values of rejection reported were 100 % for Mg(II) and 30 % for Li(I) operating at 25 bar. Werner et al. [69] studied the influence of pH for the separation of In(III) and Ge(IV) using the polyamide TFC membrane NF99HF (Alfa Laval). Authors reported an In(III) rejection of 100 % for single salt solutions of 10 mg/L of $In_2(SO_4)_3$ at pH values higher than 6. The results of In(III) rejection in this work were slightly lower, showing that the presence of other elements in brine may interfere in the rejections. In fact, ionic strength has a direct influence on pKa of species [70]. For that reason, speciation distribution of elements may vary because of the displacement of equilibrium pKa and hence, its rejections.

3.3.1. Multivalent and monovalent concentration and selectivity factors

Concentration factors of the different elements in solution were calculated (see Figs. D.1 (major elements) and D.2 (minor elements) — Supplementary Information). At 65 % p.r. only the membrane PRO-XS2 had concentration factors higher than 2 for Mg(II) in both scenarios. The PRO-XS2 also presented concentration factors higher than 2 for S(VI) in both scenarios and for Ca(II) in scenario 1 (it was about 1.9 in scenario 2). Moreover, in order to identify which membrane would provide the best selectivity in the two scenarios evaluated, selectivity factors between monovalent and multivalent elements were calculated (see Table 3). A higher selectivity among major ($\overline{SF} = 4.3$) and minor ($\overline{SF} = 38.4$) elements was achieved by PRO-XS2 operating in scenario 1. Meanwhile in scenario 2, Fortilife XC-N reached the highest selectivity among the three membranes for major elements ($\overline{SF} = 4.7$) and NF270 reported a better selectivity referred to minor elements ($\overline{SF} = 9.5$).

The values of permeate flux at initial conditions and at 65 % p.r. for the three tested membranes for both scenarios are also summarized in Table 3. The increment in permeate recovery resulted in a drop of permeate flux due to the increase of osmotic pressure in the feed side. In scenario 1, the average reduction in permeate flux was about 8 % while in brine 2 it was about 22 %. For both brines, the membrane that presented the smallest reduction was the Fortilife XC-N. Scenario 1 was expected to have a greater decrease in permeate flow due to scaling problems caused by gypsum and calcite, however a longer period of time would be needed to observe influence of scaling in reduction of permeate flow [71] since all the experiments were completed in <12 h.

Considering scenario 2, Fortilife XC-N had the highest permeate flux, the highest Ca(II) and Mg(II) rejections at 65 % p.r (about 75 % and 83 %, respectively) and major elements selectivity. However, it presented the lowest minor elements selectivity when compared to the other two membranes. It is worth mentioning that Sea4Value is interested on recovering not only minor elements but also Mg(II) and Ca(II). For scenario 1, NF270 presented the highest permeate flux but the lowest rejection of Ca(II) and Mg(II) and selectivity of major species, while PRO-XS2 presented the highest selectivity between monovalent and multivalent elements for major and minor elements but the lowest permeate flux. The economic analysis can elucidate if the difference in permeate flux between the membranes significantly affects the cost expenditures of the pre-treatment.

Table 3
Selectivity factor ($\overline{SF}$) among multivalent and multivalent elements for major and minor elements and permeate flux (Jv) at initial and final permeate recovery for the three tested membranes and the two studied scenarios.

	Scenario 1			Scenario 2		
	NF270	Fortilife XC-N	PRO-XS2	NF270	Fortilife XC-N	PRO-XS2
Selectivity factor, $\overline{SF}$						
Major	2.72 ± 0.11	3.66 ± 0.53	4.32 ± 0.29	2.42 ± 0.50	4.66 ± 0.65	3.83 ± 0.34
Minor	10.13 ± 2.47	5.51 ± 1.91	38.42 ± 15.82	9.45 ± 4.35	6.33 ± 0.69	7.07 ± 0.92
Permeate flux, J_v (LMH)						
0 % p.r	97.07	85.70	72.02	86.12	91.20	58.27
65 % p.r	90.12	83.73	61.48	66.60	73.09	45.31

3.4. Techno-economic assessment of brine pre-treatment in the Fonsalía desalination plant

The results obtained experimentally were used in the economic analysis. Hence, Table 4 collects the results of CAPEX and OPEX for each scenario and each membrane. The permeate fluxes obtained for each tested membrane (for scenario 1 and scenario 2) were used for the calculation of the number of membranes needed in each scenario. The number of membrane elements was calculated using Eq. 8 for each permeate flux reported in Table 3 (considering 65 % p.r.) and it was oversized by a 10 % as a margin of error. Besides that, it was considered that each pressure vessel contained 6 membrane elements, hence, the number of elements was adjusted to be a multiple of 6. The number of membranes needed and the total CAPEX for NF are listed in Table 4.

As the consumption of $NaHCO_3$ depends on the concentration of Ca (II) on the stream feeding the precipitation tank, for scenario 1 it was necessary to consider the Ca(II) concentration at the concentrate stream after the NF set-up for the 3 different membranes at 65 % p.r. (Section 3.1). The cost of $NaHCO_3$ related to remove Ca(II) is reported in Table 4.

The SEC of NF was calculated using Eq. 10 and resulted in 1.6 kWh/m^3. The value obtained was the same for scenarios 1 and 2 since the total permeate and feed flowrate were the same in both cases. The SEC obtained was slightly lower than the values reported in the literature for large-scale RO and NF systems, whose SEC normally varies between 2 and 4 kWh/m^3 [72]. Besides, the simulation performed with WAVE software (see Table B.1 in Supplementary Information) resulted in SEC of 1.6 and 1.7 kWh/m^3 for scenarios 1 and 2 respectively, values very close to the one obtained experimentally. With the SEC value and the permeate production of 13,650 m^3/day (Fig. 1), it was possible to calculate the NF energy consumption related to pumping requirements, as shown in Table 4 (OPEX). The cost of energy in Spain for business was considered to be 0.103 €/kWh [73].

As can be seen in Table 4, scenario 1 presented lower values of CAPEX since the size of the precipitation vessel is smaller than in scenario 2. Regarding OPEX, Table 4 presents the main expenditures excluding energy consumption of Ca(II) precipitation. The variation between scenarios is significant since the OPEX for scenario 2 is at least 40 % higher than for scenario 1. This occurred since the difference in cost of membrane replacement was not so significant as expected and the cost of chemicals represented the largest expenses. The cost of HCl consumption (only in Scenario 2) was the second highest operational expenditure excluding the energy consumption of Ca(II) precipitation. The cost of the added $NaHCO_3$ was the highest expenditure representing at least 80 % of the total OPEX and it was also higher for scenario 2. Therefore, the total levelized cost TLC that considers both OPEX and CAPEX was higher for scenario 2.

One of the critical parameters on Ca(II) removal as calcium carbonate is the temperature. Fig. 4a presents the influence of the temperature of Ca(II) precipitation in the TLC calculated for this case study and Fig. 4b presents an estimation of the variation of Ca(II) removal percentage with temperature based on Molinari et al. [20] work. The TLC at 25 °C is the one presented at Table 4 while for the other temperatures, the cost of heating the brine for Ca(II) precipitation (calculated using Aspen Hysys [74])was added.

The difference in TLC between the membranes was too small to be noticed in the graph (standard deviation between the membranes was 0.09 and 0.11 €/m^3 for scenarios 1 and 2, respectively). Hence, Fig. 4a shows only the average value of TLC for the three membranes in each scenario. PRO-XS2 presented the highest TLC in both scenarios while NF270 presented the lowest TLC in both scenarios, but Fortilife XC-N presented the same TLC of NF270 in scenario 2. Besides, Fig. 4b shows that it is possible to reach 90 % Ca(II) removal heating the brine up to 70 °C, but in Fig. 4a it is reported that this increase in temperature significantly impacts the TLC of the project. As can be seen in Fig. 4a, the temperature of Ca(II) precipitation has a greater impact on scenario 2 since the flow rate of brine feeding the precipitation stage would be higher. However, in both scenarios the cost of heating the brine can be higher than all the other expenditures considered. For example, to reach the 60 °C proposed by Molinari et al. [20] the cost of heating the brine would result in a TLC 2 times and 3 times higher for scenarios 1 and 2, respectively. Such a high TLC for the pretreatment stage alone could jeopardize the economic feasibility of the complete brine mining process. However, at room temperature the Ca(II) removal % is about 50 %. Therefore, other alternatives must be evaluated, such as increasing the pH of Ca(II) precipitation stage (authors reported that it is possible to reach a 60 % Ca(II) removal at pH 9.5) or decreasing the temperature of Ca(II) precipitation. For scenario 1 it is possible to have 80 % Ca(II) removal at 50 °C with a TLC of about 2.7 €/m^3 inlet, a value similar to the TLC for scenario 2 at room temperature. It is clear that scenario 1 would be the best option since it presented lower values of OPEX and CAPEX in all the scenarios proposed. The largest concern regarding scenario 1 was the cost of membrane replacement due to scaling in NF. However, the economic analysis showed that other expenditures were more significant.

The membrane with the highest selectivity factor between monovalent and multivalent species for scenario 1 was PRO-XS2, for minor and major elements. Although this membrane presented the lowest permeate flux resulting in the highest CAPEX and OPEX among the three

Table 4
CAPEX and OPEX for the 2 scenarios proposed in this case study, considering the 3 membranes tested and excluding energy consumption of Ca(II) precipitation.

	Scenario 1			Scenario 2		
	NF 270	Fortilife XC-N	PRO-XS2	NF 270	Fortilife XC-N	PRO-XS2
CAPEX						
Number of membrane elements	192 ± 24	222 ± 30	276 ± 42	258 ± 36	252 ± 36	378 ± 54
NF (€/(m^3/day))	151.87 ± 4.59	152.95 ± 4.73	158.43 ± 5.41	157.03 ± 5.24	155.12 ± 5.00	166.40 ± 6.40
Ca(II) precipitation (€/(m^3/day))	12.77 ± 1.60	12.77 ± 1.60	12.77 ± 1.60	21.36 ± 2.67	21.36 ± 2.67	21.36 ± 2.67
Total CAPEX (€/(m^3/day))	164.64 ± 6.19	165.72 ± 6.33	171.20 ± 7.01	178.39 ± 7.91	176.48 ± 7.67	187.76 ± 9.07
OPEX						
Membrane replacement (€/m^3)	0.008	0.008	0.010	0.007	0.005	0.009
NF energy (€/m^3)	0.11	0.11	0.11	0.11	0.11	0.11
$NaHCO_3$ (€/m^3)	1.31 ± 0.01	1.46 ± 0.01	1.46 ± 0.01	1.90 ± 0.01	1.90 ± 0.01	1.90 ± 0.01
HCl (€/m^3)	–	–	–	0.24 ± 0.004	0.24 ± 0.004	0.24 ± 0.004
Maintenance (€/m^3)	0.013 ± 0.001	0.013 ± 0.001	0.013 ± 0.001	0.014 ± 0.001	0.014 ± 0.001	0.014 ± 0.001
Labor (€/m^3)	0.025	0.025	0.025	0.025	0.025	0.025
OPEX (€/m^3)	1.46 ± 0.01	1.61 ± 0.01	1.62 ± 0.01	2.30 ± 0.01	2.30 ± 0.01	2.30 ± 0.7
Total levelized cost						
Total levelized cost (€/m^3 inlet)	1.50 ± 0.02	1.65 ± 0.02	1.66 ± 0.02	2.34 ± 0.02	2.34 ± 0.02	2.34 ± 0.02

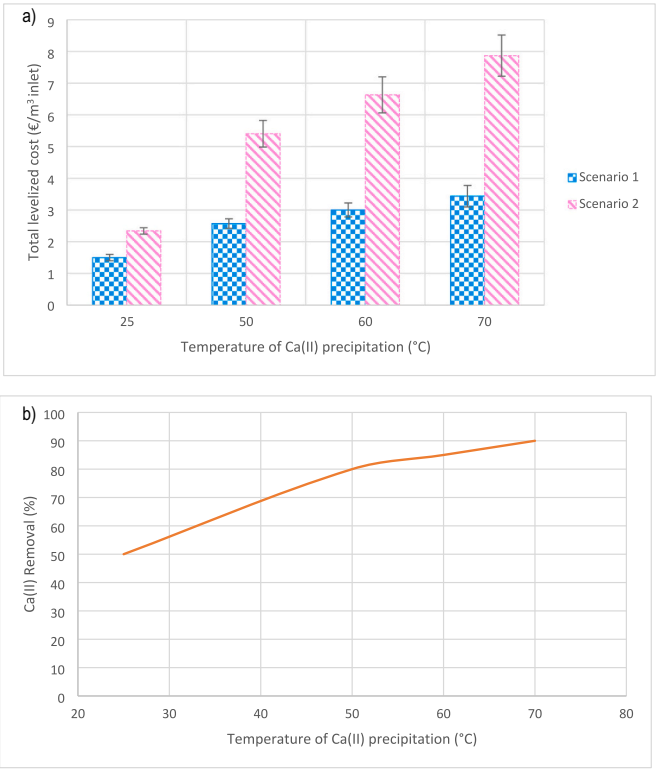

Fig. 4. Influence of the temperature of Ca(II) precipitation in a) TLC of scenarios 1 and 2 and in b) Ca(II) removal %.

membranes, this did not reflect in a big difference economically since the variation between membranes was lower than 10 % for the TLC of the pre-treatment stage. As the difference between CAPEX and OPEX is so small, membrane selectivity should be prioritized over permeate flux since higher selectivity results in higher materials recovery. For example, Mg(II) was selected as one of the elements with higher economic potential regarding SWDP brine mining [13]. As the Mg(II) recovery is designed for the concentrate stream, the amount of Mg(II) in the NF concentrate should be as high as possible. In this case, for the brine production of the Fonsalía SWDP, the NF270 membrane concentrate stream would contain about 3,000 ton Mg(II)/year less than the concentrate stream obtained by the PRO-XS2, whereas the Fortilife XC-N membrane concentrate stream would contain about 1,000 ton Mg(II)/year less than PRO-XS2. Therefore, as mentioned before, the efficiency of multivalent and monovalent separation was a priority to ensure the maximum recovery of minerals and metals from brine, hence the membrane PRO-XS2 was selected for the pre-treatment of brine coming from the Fonsalía SWDP. Table 5 collects the summary of the trade-offs between cost and membrane performance (for the best scenario) that should be considered in this case.

4. Conclusions

The lack of primary resources in the EU is promoting the need for implementing circular economy schemes, such as the recovery of raw materials from SWDP brines. However, it is necessary to pretreat such streams to maximize the recovery of these materials. This study postulates two pre-treatment scenarios based on a combination of Ca(II) removal and NF by testing three different membranes.

Overall, it was possible to verify that all the tested membranes had high rejections of multivalent elements, concentrating them in the concentrate stream, while the permeate stream was rich in monovalent elements, that were poorly rejected by the membranes. Results showed that by placing NF before Ca(II) removal unit (scenario 1), the decrease

Table 5
summary of the trade-offs between cost and membrane performance for scenario 1 at 65%p.r.

Membrane	NF 270	Fortilife XC-N	PRO-XS2
TLC (€/m^3 inlet)	1.50 ± 0.02	1.65 ± 0.02	1.66 ± 0.02
SF for minor elements	10.13 ± 2.47	5.51 ± 1.91	38.42 ± 15.82
SF for major elements	2.72 ± 0.11	3.66 ± 0.53	4.32 ± 0.29

in permeate flux when going from 0 to 65 % permeate recovery was about 8 %. Instead, by placing Ca(II) removal before NF (scenario 2), the decrease in permeate flux was about 22 %. Membranes maintained a similar selectivity factor between monovalent and multivalent species for both scenarios, except for the membrane PRO-XS2 that had a $\overline{SF}$ of minor species 5 times higher by placing NF before Ca(II) removal (scenario 1). In fact, for scenario 1 PRO-XS2 presented the highest selectivity between monovalent and multivalent for major ($\overline{SF} = 4.3$) and minor ($\overline{SF} = 38.4$) elements being the best membrane for this scenario. However, considering scenario 2, Fortilife XC-N had the highest major elements selectivity ($\overline{SF} = 4.7$) while NF270 had the highest minor elements selectivity ($\overline{SF} = 9.5$).

The economic evaluation demonstrated that scenario 1 had lower values of CAPEX since the size of the precipitation vessel is smaller in this case. Regarding OPEX, the cost of membrane replacement was not as significant as expected (below 0.02 €/m^3) while the costs of HCl consumption (about 0.24 €/m^3) and $NaHCO_3$ (at least 0.4 €/m^3 more expensive in scenario 2) contributed notably to make OPEX in scenario 2 higher than in scenario 1. On the other hand, heating the brine for Ca(II) precipitation had the greatest impact on the TLC. While the pre-treatment TLC was about 1.6 and 2.4 €/m^3 inlet for scenarios 1 and 2, respectively and considering Ca(II) precipitation at room temperature. Heating the brine to 60 °C for optimal Ca(II) removal percentage, the TLC would increase to 3.1 and 6.6 €/m^3 inlet for scenarios 1 and 2, respectively. Hence, other alternatives at lower temperature must be considered related to Ca(II) precipitation in order to decrease the TLC. All in all, scenario 1 presented lower values of CAPEX and OPEX and was selected as the best pre-treatment configuration. Furthermore, for scenario 1 the membrane PRO-XS2 was selected as the best membrane for brine pre-treatment.

CRediT authorship contribution statement

Mariana Figueira: Conceptualization, Methodology, Validation, Formal analysis, Investigation, Writing – original draft, Visualization. **Daniel Rodríguez-Jiménez:** Conceptualization, Methodology, Validation, Formal analysis, Investigation, Writing – original draft, Visualization. **Julio López:** Conceptualization, Methodology, Validation, Formal analysis, Investigation, Writing – review & editing, Visualization. **Mònica Reig:** Conceptualization, Methodology, Validation, Formal analysis, Investigation, Writing – review & editing, Visualization. **José Luis Cortina:** Conceptualization, Validation, Resources, Supervision, Funding acquisition, Writing – review & editing. **César Valderrama:** Conceptualization, Validation, Resources, Supervision, Project administration, Funding acquisition, Writing – review & editing.

Declaration of competing interest

The authors declare that they have no known competing financial interests or personal relationships that could have appeared to influence the work reported in this paper.

Data availability

The data that has been used is confidential.

Acknowledgements

This study was carried out as part of the Sea4Value project, financed by the European Union's Horizon 2020 research and innovation program under grant agreement No. 869703, which is gratefully acknowledged, and by the Catalan Government (ref. 2017-SGR-312). Additionally, the authors acknowledge the Open Innovation — Research Translation and Applied Knowledge Exchange in Practice through University-Industry Cooperation (OpenInnoTrain), Grant agreement number (GAN): 823971, H2020-MSCA-RISE-2018-823971 and the Spanish Ministry of Science and Innovation (grant agreement TED2021-131708B-C21). The authors also thank DuPont and Nitto Denko Corporation for providing the membranes for the experiments. Finally, the authors are also grateful to the editor and anonymous reviewers for their constructive criticism of the original manuscript.

Appendix A. Supplementary information

Supplementary information to this article can be found online at https://doi.org/10.1016/j.desal.2022.116321.

References

[1] European Commission, Circular Economy Action Plan For a Cleaner and More Competitive Europe, 2020.
[2] M. Azadi, S.A. Northey, S.H. Ali, M. Edraki, Transparency on greenhouse gas emissions from mining to enable climate change mitigation, Nat. Geosci. 13 (2020) 100–104, https://doi.org/10.1038/s41561-020-0531-3.
[3] European Parliament, Circular economy: definition, importance and benefits. https://www.europarl.europa.eu/news/en/headlines/economy/20151201STO05603/circular-economy-definition-importance-and-benefits, 2021 (accessed June 17, 2021).
[4] European Commission, Closing the Loop - An EU Action Plan for the Circular Economy, 2015.
[5] European Commission, Critical raw materials. https://ec.europa.eu/growth/sectors/raw-materials/areas-specific-interest/critical-raw-materials_en, 2021 (accessed November 16, 2021).
[6] M.O. Mavukkandy, C.M. Chabib, I. Mustafa, A. Al Ghaferi, F. AlMarzooqi, Brine management in desalination industry: from waste to resources generation, Desalination 472 (2019), 114187, https://doi.org/10.1016/j.desal.2019.114187.
[7] IDA, GWI DesalData, The IDA Water Security Handbook 2019–2020, 2019.
[8] A. Pérez-González, A.M. Urtiaga, R. Ibáñez, I. Ortiz, State of the art and review on the treatment technologies of water reverse osmosis concentrates, Water Res. 46 (2012) 267–283, https://doi.org/10.1016/j.watres.2011.10.046.
[9] Sea4Value, The Project - Sea4value. https://sea4value.eu/the-project/, 2020 (accessed January 14, 2021).
[10] C. Liu, B. Tao, Z. Wang, D. Wang, R. Guo, L. Chen, Preparation and characterization of lithium ion sieves embedded in a hydroxyethyl cellulose cryogel for the continuous recovery of lithium from brine and seawater, Chem. Eng. Sci. 229 (2021), https://doi.org/10.1016/j.ces.2020.115984.
[11] G. Naidu, S. Jeong, Y. Choi, M.H. Song, U. Oyunchuluun, S. Vigneswaran, Valuable rubidium extraction from potassium reduced seawater brine, J. Clean. Prod. 174 (2018) 1079–1088, https://doi.org/10.1016/j.jclepro.2017.11.042.
[12] M. Figueira, M. Reig, M. Fernández de Labastida, J.L. Cortina, C. Valderrama, Boron recovery from desalination seawater brines by selective ion exchange resins, J. Environ. Manag. 314 (2022), 114984, https://doi.org/10.1016/j.jenvman.2022.114984.
[13] A. Kumar, G. Naidu, H. Fukuda, F. Du, S. Vigneswaran, E. Drioli, J.H. Lienhard, Metals recovery from seawater desalination brines: technologies, opportunities, and challenges, ACS Sustain. Chem. Eng. 9 (2021) 7704–7712, https://doi.org/10.1021/acssuschemeng.1c00785.
[14] A. Khalil, S. Mohammed, R. Hashaikeh, N. Hilal, Lithium recovery from brine: recent developments and challenges, Desalination 528 (2022), https://doi.org/10.1016/j.desal.2022.115611.
[15] A. Shahmansouri, J. Min, L. Jin, C. Bellona, Feasibility of extracting valuable minerals from desalination concentrate: a comprehensive literature review, J. Clean. Prod. 100 (2015) 4–16, https://doi.org/10.1016/j.jclepro.2015.03.031.
[16] J. López, M. Reig, O. Gibert, J.L.L. Cortina, Integration of nanofiltration membranes in recovery options of rare earth elements from acidic mine waters, J. Clean. Prod. 210 (2019) 1249–1260, https://doi.org/10.1016/j.jclepro.2018.11.096.
[17] M.E.A. Ali, Nanofiltration process for enhanced treatment of RO brine discharge, Membranes (Basel) 11 (2021), https://doi.org/10.3390/membranes11030212.
[18] F. Du, D.M. Warsinger, T.I. Urmi, G.P. Thiel, A. Kumar, J.H. Lienhard, Sodium hydroxide production from seawater desalination brine: process design and energy efficiency, Environ. Sci. Technol. 52 (2018) 5949–5958, https://doi.org/10.1021/acs.est.8b01195.
[19] A. Giwa, V. Dufour, F. al Marzooqi, M. al Kaabi, S.W. Hasan, Brine management methods: Recent innovations and current status, Desalination 407 (2017) 1–23, https://doi.org/10.1016/J.DESAL.2016.12.008.
[20] R. Molinari, A.H. Avci, P. Argurio, E. Curcio, S. Meca, M. Plà-Castellana, J. L. Cortina, Selective precipitation of calcium ion from seawater desalination reverse osmosis brine, J. Clean. Prod. 328 (2021), 129645, https://doi.org/10.1016/j.jclepro.2021.129645.
[21] J. Zhao, M. Wang, H.M.S. Lababidi, H. Al-Adwani, K.K. Gleason, A review of heterogeneous nucleation of calcium carbonate and control strategies for scale formation in multi-stage flash (MSF) desalination plants, Desalination 442 (2018) 75–88, https://doi.org/10.1016/J.DESAL.2018.05.008.
[22] Y. Wang, Y. Qin, B. Wang, J. Jin, B. Wang, D. Cui, Selective removal of calcium ions from seawater or desalination brine using a modified sodium carbonate method, Desalin. Water Treat. 174 (2020) 123–135, https://doi.org/10.5004/dwt.2020.24828.
[23] N.Chrisayu Natasha, L.Hanum Lalasari, Calcium extraction from brine water and seawater using oxalic acid, AIP Conf Proc. (2017), https://doi.org/10.1063/1.4974443.
[24] W. Mickols, Z. Mai, B. van der Bruggen, Effect of pressure and temperature on solvent transport across nanofiltration and reverse osmosis membranes: an activity-derived transport model, Desalination 501 (2021), https://doi.org/10.1016/j.desal.2020.114905.
[25] Aguas Residuales, Estación Desaladora de Agua de Mar - EDAM de Fonsalía en Tenerife. https://www.aguasresiduales.info/revista/videos/estacion-desaladora-de-agua-de-mar-edam-de-fonsalia-en-tenerife-jwzY6, 2018 (accessed February 24, 2022).
[26] J. Eke, A. Yusuf, A. Giwa, A. Sodiq, The global status of desalination: an assessment of current desalination technologies, plants and capacity, Desalination 495 (2020), 114633, https://doi.org/10.1016/j.desal.2020.114633.
[27] B. Sauvet-Goichon, Ashkelon desalination plant - a successful challenge, Desalination 203 (2007) 75–81, https://doi.org/10.1016/j.desal.2006.03.525.
[28] ACWA Power, RABIGH 3 IWP. acwapower.com/en/projects/rabigh-3-iwp/, 2022 (accessed November 10, 2022).
[29] C.S. Nnebuo, D. Hambsch, O. Nir, Elucidating morphological effects in membrane mineral fouling using real-time particle imaging and impedance spectroscopy, Environ. Sci. (Camb) (2022) 1–40, https://doi.org/10.1039/D2EW00155A.
[30] I. Puigdomenech, Chemical equilibirum software Hydra/Medusa. https://sites.google.com/site/chemdiagr/home, 2001.
[31] N. Melián-Martel, J.J.Sadhwani Alonso, S.O.Pérez Báez, Reuse and management of brine in sustainable SWRO desalination plants, Desalination Water Treat. 51 (2013) 560–566, https://doi.org/10.1080/19443994.2012.713567.
[32] M. Petersková, C. Valderrama, O. Gibert, J.L. Cortina, Extraction of valuable metal ions (Cs, rb, li, U) from reverse osmosis concentrate using selective sorbents, Desalination 286 (2012) 316–323, https://doi.org/10.1016/j.desal.2011.11.042.
[33] H.S. Son, S. Soukane, J. Lee, Y. Kim, Y.-D. Kim, N. Ghaffour, Towards sustainable circular brine reclamation using seawater reverse osmosis, membrane distillation and forward osmosis hybrids: an experimental investigation, J. Environ. Manag. 293 (2021), 112836, https://doi.org/10.1016/j.jenvman.2021.112836.
[34] DuPont, Water Application Value Engine (WAVE), 2022.
[35] R.W. Baker, Membrane Technology and Applications, Third Edition, John Wiley & Sons, Ltd., 2012. www.wiley.com.
[36] M. Adel, T. Nada, S. Amin, T. Anwar, A.A. Mohamed, Characterization of fouling for a full-scale seawater reverse osmosis plant on the Mediterranean Sea: membrane autopsy and chemical cleaning efficiency, Groundw. Sustain. Dev. 16 (2022), 100704, https://doi.org/10.1016/j.gsd.2021.100704.
[37] R.Y. Ning, Desalination Updates, INTECH, 2015.
[38] Spanish national institute of statistics, Indice de precios de consumo. Base 2021. Medias anuales. ine.es/jaxiT3/Tabla.htm?t=50934&L=0, 2022 (accessed November 6, 2022).
[39] D.R. Woods, Rules of Thumb in Engineering Practice, WILEY-VCH, Weinheim, 2007.
[40] DuPont, FilmTecTM NF270-400/34i Element, 2021. www.dupont.com/water/contact-us.
[41] Hydranautics, PRO-XS2, PRO-XS3, 2020.
[42] DuPont, FilmTecTM FortilifeTM XC-N Element. www.dupont.com/water/contact-us, 2020.
[43] Q. Chen, M. Burhan, M.W. Shahzad, D. Ybyraiymkul, F.H. Akhtar, Y. Li, K.C. Ng, A zero liquid discharge system integrating multi-effect distillation and evaporative crystallization for desalination brine treatment, Desalination 502 (2021), https://doi.org/10.1016/j.desal.2020.114928.
[44] S. Jiang, Y. Li, B.P. Ladewig, A review of reverse osmosis membrane fouling and control strategies, Sci. Total Environ. 595 (2017) 567–583, https://doi.org/10.1016/J.SCITOTENV.2017.03.235.
[45] P.J. Brown, C.L. Cox, Filtration of drinking water, in: Fibrous Filter Media, Elsevier, 2017, pp. 245–272.
[46] K.C. Sole, A. Prinsloo, E. Hardwick, Recovery of copper from Chilean mine waste waters, Freiberg, in: Mining Meets Water - Conflicts and Solutions, 2016, pp. 1295–1302.
[47] N.S. Siefert, S. Litster, Exergy and economic analyses of advanced IGCC-CCS and IGFC-CCS power plants, Appl. Energy 107 (2013) 315–328, https://doi.org/10.1016/j.apenergy.2013.02.006.
[48] Banco de España, Tabla tipos de interés legal - Cliente Bancario. https://clientebancario.bde.es/pcb/es/menu-horizontal/productosservici/relacionados/tiposinteres/guia-textual/tiposinteresrefe/Tabla_tipos_de_interes_legal.html, 2022 (accessed April 19, 2021).

[49] M. Wenzlick, N. Siefert, Techno-economic analysis of converting oil & gas produced water into valuable resources, Desalination 481 (2020), https://doi.org/10.1016/j.desal.2020.114381.
[50] A.S. Stillwell, M.E. Webber, Predicting the specific energy consumption of reverse osmosis desalination, Water (Switzerland) 8 (2016), https://doi.org/10.3390/w8120601.
[51] Z. Wang, Y. Zhang, T. Wang, B. Zhang, H. Ma, Design and energy consumption analysis of small reverse osmosis seawater desalination equipment, Energies (Basel) 14 (2021), https://doi.org/10.3390/en14082275.
[52] A. Panagopoulos, Beneficiation of saline effluents from seawater desalination plants: fostering the zero liquid discharge (ZLD) approach - a techno-economic evaluation, J. Environ. Chem. Eng. 9 (2021), https://doi.org/10.1016/j.jece.2021.105338.
[53] COGERSA, Ajudicación del contrato de suministro de diversos reactivos químicos. https://cogersasau.sedelectronica.es/, 2021.
[54] Chemanalyst, Hidrochloric Acid Price Trend and Forecast. chemanalyst.com/Pricing-data/hydrochloric-acid-61, 2022 (accessed May 19, 2022).
[55] FEIQUE, in: XIX Convenio General de la Indsutria Química, 2019, p. 151.
[56] A. Kaya, M. Evren Tok, M. Koc, A levelized cost analysis for solar-energy-powered sea water desalination in the Emirate of Abu Dhabi, Sustainability (Switzerland) 11 (2019), https://doi.org/10.3390/su11061691.
[57] M. Reig, S. Casas, O. Gibert, C. Valderrama, J.L. Cortina, Integration of nanofiltration and bipolar electrodialysis for valorization of seawater desalination brines: production of drinking and waste water treatment chemicals, Desalination 382 (2016) 13–20, https://doi.org/10.1016/j.desal.2015.12.013.
[58] P. Ortiz-albo, R. Ibañez, A. Urtiaga, I. Ortiz, Separation and Puri fi cation technology phenomenological prediction of desalination brines nano filtration through the indirect determination of zeta potential, Sep. Purif. Technol. 210 (2019) 746–753, https://doi.org/10.1016/j.seppur.2018.08.066.
[59] M. Micari, D. Diamantidou, B. Heijman, M. Moser, A. Haidari, H. Spanjers, V. Bertsch, Experimental and theoretical characterization of commercial nanofiltration membranes for the treatment of ion exchange spent regenerant, J. Membr. Sci. 606 (2020), 118117, https://doi.org/10.1016/j.memsci.2020.118117.
[60] A.E. Yaroshchuk, Dielectric exclusion of ions from membranes, Adv. Colloid Interf. Sci. 85 (2000) 193–230.
[61] Y. Boussouga, H. Than, A.I. Schäfer, Selenium species removal by nano filtration: determination of retention mechanisms, Sci. Total Environ. 829 (2022), 154287, https://doi.org/10.1016/j.scitotenv.2022.154287.
[62] A. Werner, A. Rieger, M. Mosch, R. Haseneder, J.U. Repke, Nanofiltration of indium and germanium ions in aqueous solutions: influence of pH and charge on retention and membrane flux, Sep. Purif. Technol. 194 (2018) 319–328, https://doi.org/10.1016/j.seppur.2017.11.006.
[63] E. Van Eynde, L. Weng, R.N.J. Comans, Applied geochemistry boron speciation and extractability in temperate and tropical soils: a multi-surface modeling approach, Appl. Geochem. 123 (2020), 104797, https://doi.org/10.1016/j.apgeochem.2020.104797.
[64] A.E. Yaroshchuk, Negative rejection of ions in pressure-driven membrane processes, Adv. Colloid Interf. Sci. 139 (2008) 150–173, https://doi.org/10.1016/j.cis.2008.01.004.
[65] J. Liu, J. Yuan, Z. Ji, B. Wang, Y. Hao, X. Guo, Concentrating brine from seawater desalination process by nanofiltration-electrodialysis integrated membrane technology, Desalination 390 (2016) 53–61, https://doi.org/10.1016/j.desal.2016.03.012.
[66] S. El-ghzizel, H. Zeggar, M. Tahaikt, F. Tiyal, A. Elmidaoui, Nanofiltration process combined with electrochemical disinfection for drinking water production: feasibility study and optimization, J. Water Process Eng. 36 (2020), https://doi.org/10.1016/j.jwpe.2020.101225.
[67] P. Nativ, O. Leifman, O. Lahav, R. Epsztein, Desalinated brackish water with improved mineral composition using monovalent-selective nanofiltration followed by reverse osmosis, Desalination 520 (2021), 115364, https://doi.org/10.1016/j.desal.2021.115364.
[68] A. Somrani, A.H. Hamzaoui, M. Pontie, Study on lithium separation from salt lake brines by nanofiltration (NF) and low pressure reverse osmosis (LPRO), Desalination 317 (2013) 184–192, https://doi.org/10.1016/j.desal.2013.03.009.
[69] A. Werner, A. Rieger, M. Mosch, R. Haseneder, J.U. Repke, Nanofiltration of indium and germanium ions in aqueous solutions: influence of pH and charge on retention and membrane flux, Sep. Purif. Technol. 194 (2018) 319–328, https://doi.org/10.1016/j.seppur.2017.11.006.
[70] L. Samuelsen, R. Holm, A. Lathuile, C. Schönbeck, Buffer solutions in drug formulation and processing: how pKa values depend on temperature, pressure and ionic strength, Int. J. Pharm. 560 (2019) 357–364, https://doi.org/10.1016/j.ijpharm.2019.02.019.
[71] C.A.C. van de Lisdonk, J.A.M. van Paassen, J.C. Schippers, Monitoring scaling in nanofiltration and reverse osmosis membrane systems, Desalination 132 (2000) 101–108, https://doi.org/10.1016/S0011-9164(00)00139-9.
[72] A. Shrivastava, D. Stevens, Energy efficiency of reverse osmosis, in: Sustainable Desalination Handbook: Plant Selection, Design and Implementation, 2018, pp. 25–54.
[73] Global Petrol Prices, Spain electricity prices. https://www.globalpetrolprices.com/Spain/electricity_prices/, 2021 (accessed March 13, 2022).
[74] The Aspen Institute, Aspen Hysys, College Excellence Program, 2017.